Development of Engineered Biochar Cocktails for Odor Removal in Composting Facilities

Yaime Jefferson Milan, Manuel Garcia–Perez

Biological Systems Engineering, Washington State University, Pullman, WA 99164, USA

A report for
The Waste to Fuels Technology Partnership
2019-2021 Biennium: Advancing Organics Management in Washington State

Center for
Sustaining Agriculture
& Natural Resources
WASHINGTON STATE UNIVERSITY

DEPARTMENT OF
ECOLOGY
State of Washington

June 2021

Table of Contents

Figures

Tables

Abstract

Biochar can be used to remove odorous or toxic compounds, where these gaseous emissions (and others) are an environmental concern and a potential risk to human health. Engineered biochars have the potential to out-perform non-engineered biochars in capturing gaseous emissions, though performance is specific to the gas being managed. We developed and evaluated engineered biochars that could be used to capture certain gases emitted during the composting process.

Twelve biochar samples were produced from the pyrolysis of wheat straw (WS) and Douglas fir (DF) biomass at either 400º or 600º C in a furnace tube reactor. N doped char was produced under the presence of ammonia, and Mg-N doped char was obtained by impregnating the biomass with $MgCl_2 \bullet 6H_2O$, and using ammonia as an activating agent in the pyrolysis process. A characterization of the carbonaceous material was performed by elemental analysis, proximate analysis, gas physisorption analysis, Fourier Transform Infrared Spectroscopy (FTIR) and calculating the pH. For all the biochar samples studied, the carbon content, ash content, volume of micropores and pH values increased with the pyrolysis temperature. Due to the presence of Mg, which blocks the pores of the biochar, the surface area for the Mg-doped biochar decreased in comparison to the raw and N doped biochar.

Adsorption tests were performed to measure the capacity of the different biochar to capture H_2S, NH_3 and CO_2. More studies are underway with other gases released during composting (CH_4 and N_2O). These gases are present in composting emissions. H_2S and CO_2 adsorption experiments showed that the surface area, pH, and nitrogen content have a strong influence in the performance of biochar to remove these pollutants. For NH_3, the acidic functional groups on the adsorbent surface were the main factor determining adsorbtion and removal. Based on this work, additional studies are underway with methane and nitrous oxide, two other gases released during composting.

If biochar were used at composting facilities to capture gaseous emissions, more than one compound would likely be targeted. Thus, a blend of biochars would be necessary. Based on the adsorption capacities obtained for H_2S, and additional results found in the literature, a blend of different biochars is a still a promising concept. To develop viable biochar mixtures that could be added to composts for control of gaseous emissions, other activation strategies need to be explored for the feedstocks available in the Pacific Northwest to obtain stronger adsorption performance.

Introduction

Solid organic waste management is a challenge worldwide. Several technologies, including anaerobic digestion and composting, utilize microorganisms to process solid organic waste into more stable and environmentally friendly products that may be utilized by diversified end-markets including landscaping and agriculture (Font, et al., 2011).

Composting is widely used in Washington State and throughout the U.S. to sustainably manage organics. In 2019, there were approximately 66 compost facilities in Washington State, composting a total of nearly 1.4 million tons of material (Ecology, 2019). As the amounts of organic and food wastes diverted to composting facilities has risen in recent years, some facilities have increased the emission of odors. Emissions of concern can include nitrogen-based compounds, sulfur-based compounds, and volatile organic compounds (VOCs) (Font, et al., 2011; Eitzer, 1995). VOCs are organic chemicals with higher vapor pressures and malodorous and hazardous properties (Dhamodharan, 2019; Komilis, et al., 2004). Certain VOCs are carcinogens, and can directly affect human health.

The composting process is aerobic; however anaerobic conditions exist in some parts of the piles (Dhamodharan, 2019). During composting, carbon dioxide (CO_2)is released under aerobic conditions, while CH_4 (methane), H_2S (hydrogen sulfide) and N_2O (nitrous oxide) are generated under anaerobic conditions. The carbon dioxide from composting is not normally considered a greenhouse gas emission because it is of recent origin from living material. However, its retention in finished compost could enhance carbon sequestration, an important avenue for reducing greenhouse gas emissions. Methane and nitrous oxide are powerful greenhouse gases that contribute to climate change. Meanwhile, H_2S is a common, dangerous, and odorous compound. Organic wastes emit variable amounts of CO_2, CH_4, and N_2O based on their C and N content and the conditions under which the composting process is managed (Swati & Hait, 2018).

Composting operations have a handful of methods available to control odor (Ma et al. 2013). Among these methods, it is critical to ensure that conditions in the composting piles remain aerobic to avoid the formation of malodorus products released under anaerobic conditions. This is achieved by blending adequate lignocellulosic materials (e.g. wood, dry plant matter, other bulking materials) with wet materials (e.g. food wastes). Appropriately controlling the air supply can also be important to maintaining aerobic conditions.

As an additional control, some facilities also use biofilters and biocovers to adsorb offensive odors. Within these filters, molecules responsible for unpleasant odors are metabolised by bacteria. The main challenge of existing biofilters is the need to keep them wet, and maintaining the filters to work effectively.

If appropriately engineered, biochar may provide an additional tool in the future for managing gaseous emissions (Sánchez-Monedero, et al., 2019). Biochar is a carbonaceous solid product derived from the thermochemical decomposition of wood or other organic matter in the absence of, or with restricted amounts of, oxygen (Lehmann & Joseph, 2015). In contrast to biofilters, biochar use could be applicable in situations in which the air pipe and the fans deliver air into the pile and the odors are released to the surrounding environment. Blending the right quantities of

engineered chars with the composting materials should be able to retain most of the odors released by the composting facility.

The objective of this research was to identify production conditions for creating biochar with an enhanced capacity to adsorb some common air pollutants released during biomass composting in municipal solid waste composting facilities. Because of the diversity of the contaminants released during biomass composting, it is unlikely that a single type of biochar will be able to adsorb all of the contaminants, so the development of biochar mixtures was expected to be more effective. This research focused on three common pollutants – CO_2, H_2S and NH_3 – as a first step towards understanding how biochar, and cocktails of various types of biochar, can be used to adsorb emissions.

This research was completed using the following steps:

1. Production of 12 types of engineered biochar under various conditions.
2. Characterizations of the resulting biochar
    a. elemental composition: to determine the C, H, N and O composition of the biochar samples
    b. proximate analysis: to determine the volatile composition, fixed carbon content, ash content and composition, and moisture content of the biochar samples
    c. gas physiosorption analysis: utilizing CO_2 adsorption to determine surface area and pore size of the biochar samples
    d. Fourier-transform infrared spectroscopy: to identify the functional groups on the surface and within the char to analyse the potential ability to adsorb various contaminants
    e. pH analysis: to assess the pH of the biochar samples
3. H_2S, CO_2, and NH_3 adsorption studies to evaluate the ability of each type of biochar to adsorb these targeted pollutants.
4. Based on the results from step 3, explore the use of a cocktail blend of biochar that can remove the pollutants in a composting facility.

Methods and Materials

Biochar preparation

Wheat straw (WS) and Douglas fir (DF) (*Pseudotsuga menziesii)* biomass feedstock were chosen to produce the biochars based on their availability in Washington State, and their common use for biochar production. The feedstocks, which were obtained from Green Stripe brand wheat straw (WS) and forestry residuals (DF), were washed and oven-dried at a temperature of 105ºC for 24 hours, and then ground below 2.5 mm sieve size by a blade grinder (KRUPS F203 Electric spice and coffee grinder with stainless steel blades). The particles of the resulting samples were

separated using a U.S. Standard Sieve Series to capture particles between 1.168 mm and 0.60 mm.

Biochar production and physical/chemical activation

Twelve different samples of biochar were produced from WS and DF at two different temperature (400℃ and 600℃) using a Quartz Tube furnace reactor of 50 OD×44 ID×1000 L, mm (2"D×40"L). The 12 samples are shown below in Table 1, with the temperature at which they were produced.

Table 1: A summary of the 12 types of biochar samples produced from Douglas fir (DF) or wheat straw (WS) biomass.

Biochar sample	Temperature (℃)
WS Raw	400
WS Raw	600
WS N-doped	400
WS N-doped	600
WS N-Mg doped	400
WS N-Mg doped	600
DF Raw	400
DF Raw	600
DF N-doped	400
DF N-doped	600
DF N-Mg doped	400
DF N-Mg doped	600

N doping

To produce biochar samples doped with nitrogen (N), the following pyrolysis process was used: Approximately 3 grams of biomass (DF or WS) were placed in the reactor in an N_2 atmosphere (oxygen-free) as the temperature was raised to 400℃ or 600℃, then maintained at that temperature for one hour under N_2 gas (the carbonization process). The biochar was then treated at the same temperature with NH_3 (ammonia) for 1 hour to produce nitrogen-doped biochar (the doping process). Samples were then cooled to 25°C in nitrogen gas. The flow rates of gas used in the process were of 500 mL min^{-1} for the N_2 and NH_3 conditions.

N-Mg doping

The Mg-impregnated biochar was prepared by first mixing 10 grams of DF or WS biochar with 40 mL of $MgCl_2 \cdot 6H_2O$ solution, prepared by dissolving 16.75 g of $MgCl_2 \cdot 6H_2O$ in 100 mL of deionized water at room temperature. Then, the steps outlined above for N doping were followed.

The biochars obtained were then characterized and used for the adsorption studies.

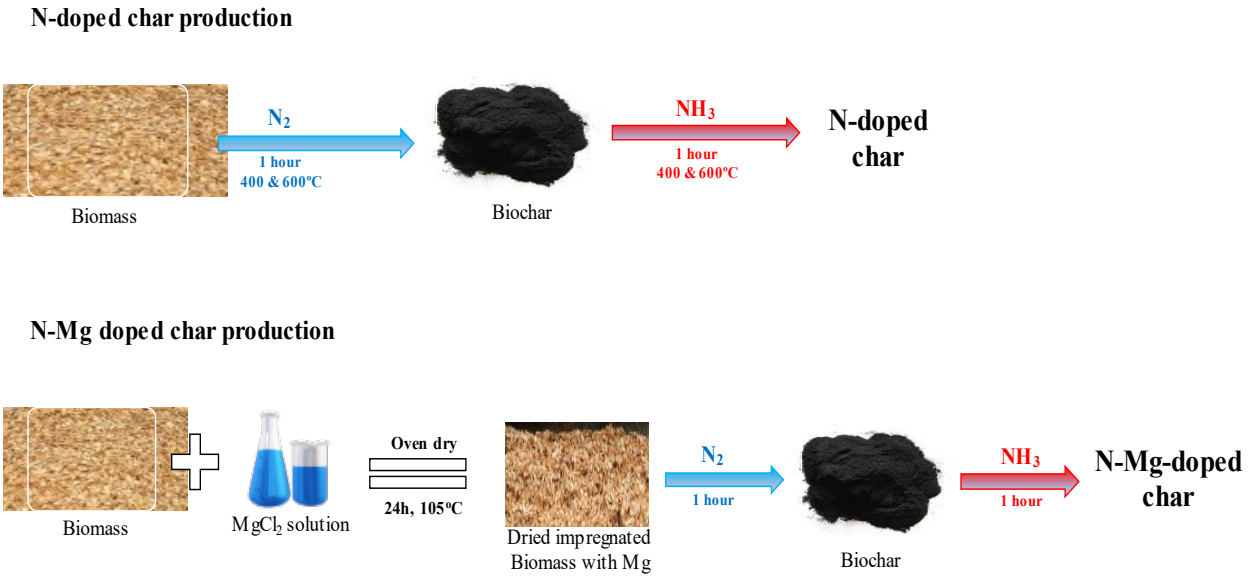

Figure 1: Nitrogen doped and Nitrogen-Mg doped biochar production steps.

Biochar characterization

Following production of the 12 samples of biochar (see Table 1), the following characterization methods were utilized on each sample type.

Elemental analysis

To determine the C, H, N and O composition of the biochar samples, a TRUSPEC-CHN® (LECO, US) elemental analyzer was used to complete the elemental analysis described by (Suliman et al., 2016a). A .15g biochar sample was used to determine total C, N, and H content. The oxygen mass fraction was determined by subtracting the ash, C, N, and H contents from 1.

Proximate analysis

The proximate analysis determines the moisture content, fixed carbon, volatiles, and ash content of the biochar samples, using a thermogravimetric analyzer (TGA) SDTA851e (Mettler Toledo, US) and following the methods described by (Ayiania, et al., 2019). The moisture content was determined as the weight loss after 0.5g of biochar was heated in a crucible from 25°C to 120°C

and held at this temperature for 3 min under nitrogen gas. After this, the temperature was increased from 120°C to 950°C (under nitrogen), and held for 5 min to determine the volatile matter. The temperature was then decreased from 950°C to 450°C, placed under oxygen flow, and heated from 450°C to 600°C and held for 8 min to obtain the ash mass.

Gas physisorption analysis

The gas physiosorption analysis uses CO_2 to determine the surface area and pore size. This analysis uses a Micromeritics TriStar II 3030 PLUS Surface Area and Porosity Analyzer (Norcross, GA, USA) to obtain the CO_2 adsorption isotherms at 273 K. Biochar samples (0.1 g) were used to perform the analysis. The samples were degassed at 200°C for 18 h under a vacuum of about 0.05-0.1 mbar (the degassing temperature was chosen based on the production temperature of the biochar to avoid sample degradation during preparation).

CO_2 adsorption isotherms were measured between the partial pressure range of $p/p_o = 10^{-5}$ to $p/p_o = 0.03$ using 75 set equilibration points. Surface area and micropore volumes were estimated using the Dubin–Radushkevich (DR) equation. Density functional theory (DFT) calculations were carried out to calculate the pore size distribution assuming a slit pore shape (Suliman, et al., 2016a).

Fourier Transform Infrared Spectroscopy (FTIR)

A Fourier-transform infrared spectroscopy analysis identifies functional groups on the surface and within the biochar samples to analyze the potential ability to adsorb various pollutants. To obtain an infrared spectrum of absorption of the biochar, a Shimadzu IRPrestige 21 spectrometer equipped with a "MIRacle single reflection ATR Ge probe" was used to determine the FTIR spectra for all the biochar to identify the functional groups present in the samples. The chars were placed to cover the crystal window and the FTIR spectrum was recorded between 4000 and 400 cm^{-1}. 64 scans were performed per sample (Ayiania, et al., 2020).

pH analysis

The pH of the biochar samples (an important factor in the ability to adsorp pollutants) was determined using the methods described by (Wang, et al., 2012; Cantrell, et al., 2012). A suspension of biochar in deionized water with a ratio of 1:100 w/v was prepared and mechanically shaken at 140 rpm for 2 hours at room temperature (25°C). The suspension was allowed to stand for 30 minutes, and then the pH values were measured using a Mettler Toledo SevenEasy S20 pH Meter.

Adsorption studies

H_2S and CO_2 adsorption

Adsorption tests were performed in vertically oriented polycarbonate tubes, at atmospheric pressure and room temperature conditions. The amount of biochar used in each test was 0.3 grams and 5.0 grams for the H_2S and CO_2 adsorption studies, respectively.

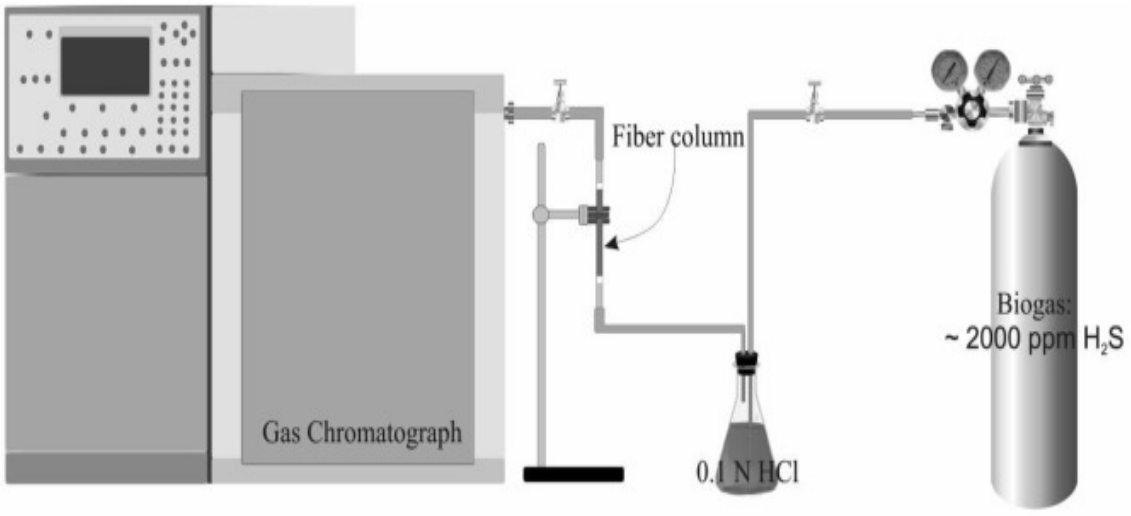

Figure 2: The experimental setup to study biochar adsorption capacity for H_2S (Ayiania, et al., 2019).

Simulated biogas containing 2000 ppm of H_2S or 348000 ppm CO_2 were used for each adsorption trial. The gases passed through the column of adsorbent biochar at a flow rate of 8 mL min−1 for H_2S and 0.30 mL min−1 for CO_2, controlled by a volumetric flow meter device. A 0.1 N HCl solution was utilized to humidify the biogas before reaching the column of biochar. The concentration in the outlet was measured every 10 minutes using a gas chromatography analyzer (GC; Varian GC3800, equipped with an Agilent CP-SilicaPLOT 50 m×0.53 mm x 4 μm column) with a computer-automated data acquisition program (Ayiania, et al., 2019). The breakthrough concentration was set when the first non-zero H_2S concentration was detected at the outlet of the biochar column.

NH_3 adsorption

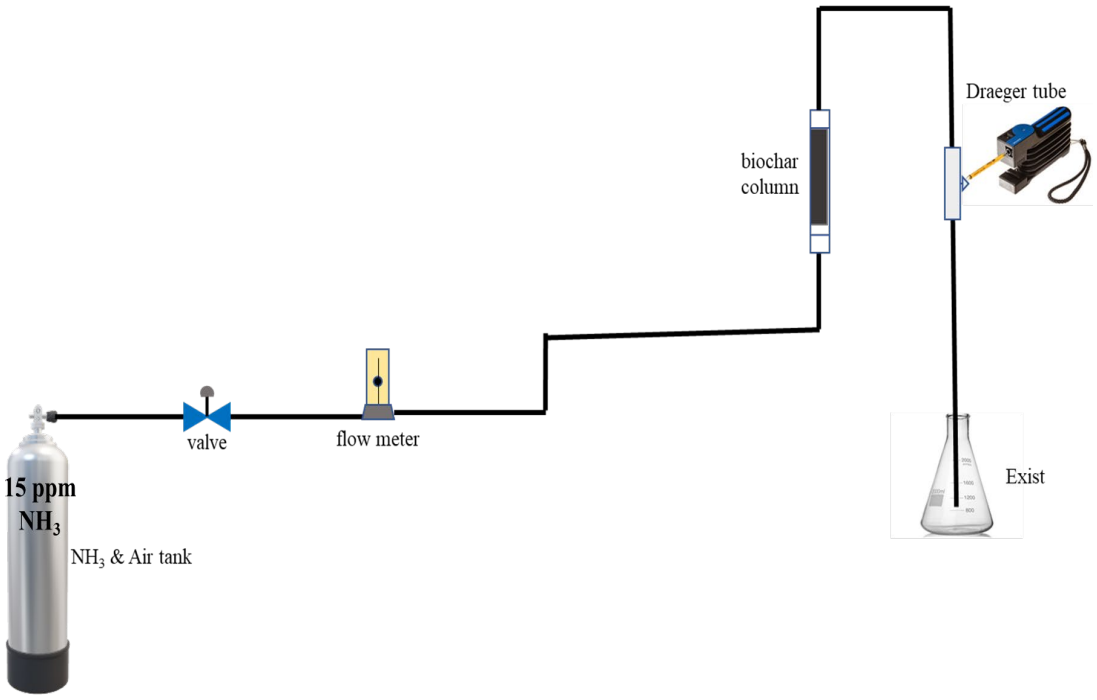

Figure 3: Experimental set up to study biochar adsorption capacity for NH_3.

The experiments were carried out in vertically oriented polycarbonate tubes filled with 0.45 grams of biochar and were conducted by passing 15ppm NH_3 gas through a column of biochar at a rate of 60 mL/min as shown in Figure 3. The NH_3 concentration at the outlet of the column was measured every 10 minutes by a gas-detecting tube technique (Ammonia 2/a 6733231 Draeger Tube, measuring range: 2 – 30 ppm), and the breakthrough concentration was determined when the first non-zero NH_3 concentration was detected at the outlet of the biochar column.

The adsorption capacity (mg/g) for the gases were calculated using the following equation:

$$\mathbf{q_t} = \frac{\boldsymbol{F}}{\boldsymbol{m}} \int_0^t (\mathbf{C_0} - \mathbf{C_t})\, \boldsymbol{dt}$$

Where: C_0 (mg/mL) and C_t (mg/mL) are the gas concentrations initially and at time t (min), F (mL/min) is the flow rate, m (g) the mass of biochar, t (min) is the time and q_t is the adsorption capacity (mg gas/g biochar) (Yang, et al., 2019; Rodrigues, et al., 2007).

Statistical analysis

The statistical software SAS University Edition (version 3.8) was used to perform statistical analysis for all the biochar characterization and adsorption experiments. The statistical analyses were done in triplicate. Determination of the standard deviation, sample means, and t- test were completed using a 0.05 significance level. The correlation analysis was done using the statistical software JMP Pro 12.

Results and Discussion

Biochar characterization

Biochar yield

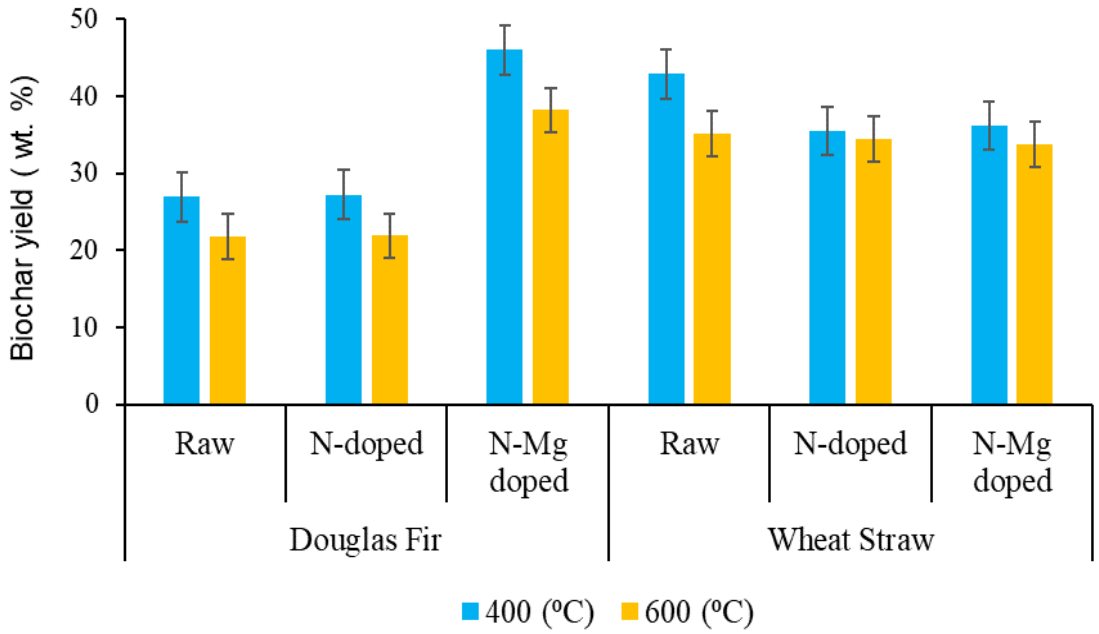

Figure 4 shows the yield of biochar obtained from the wheat straw and Douglas fir biomass. The biochar yield decreased as the production temperature increased from 400°C to 600°C, which can be attributed to the reduction of C, H, and O as volatile gases by the pyrolysis reactions (Suliman, et al., 2016b). The yields of biochars are dependent on the feedstock properties. WS biochars produced from raw biomass and doped with nitrogen resulted in a higher yield than the biochar obtained from DF at the same conditions, because WS feedstock has more ash content than DF, which contributed to biochar formation. The yield of DF N-Mg doped biochar is greater that that of WS N-Mg, mainly due to the presence of alkali and alkaline earth metals (Mg, Ca, K)

that can catalyze biomass decomposition and promote the formation of biochar (Zhang, et al., 2018).

Elemental analysis

The elemental composition of the biochars produced at different pyrolysis temperatures is shown in Table 2. Increasing the pyrolysis temperature from 400℃ to 600℃ increased the C content for all biochar, however, the H and O mass fraction decreased due to the bond-breaking reactions that form volatile species, which escape with the increase of the temperature.

Table 2: Elemental composition of biochar produced at different temperatures.

Dry basis	Temperature (℃)	Carbon (wt. %)	Hydrogen (wt. %)	Nitrogen (wt. %)	Oxygen (wt. %)
WS Raw	400	70.2 ± 0.10	3.7 ± 0.003	0.8 ± 0.09	8.0 ± 0.62
WS Raw	600	71.6 ± 0.45	1.4 ± 0.02	0.7 ± 0.04	7.6 ± 0.91
WS N-doped	400	63.6 ± 0.23	2.4 ± 0.47	0.9 ± 0.10	12.7 ± 0.09
WS N-doped	600	69.2 ± 0.45	1.4 ± 0.12	5.3 ± 0.20	2.0 ± 0.97
WS N-Mg doped	400	26.3 ± 0.17	1.6 ± 0.04	1.0 ± 0.02	40.1 ± 0.61
WS N-Mg doped	600	27.5 ± 0.17	0.7 ± 0.01	5.2 ± 0.09	25.2 ± 0.74
DF Raw	400	84.1 ± 0.07	4.2 ± 0.01	0.3 ± 0.03	11.0 ± 0.14
DF Raw	600	93.7 ± 0.29	2.6 ± 0.03	0.5 ± 0.02	2.3 ± 0.15
DF N-doped	400	84.2 ± 0.01	4.1 ± 0.08	1.2 ± 0.03	10.1 ± 0.06
DF N-doped	600	93.7 ± 0.06	2.4 ± 0.01	1.7 ± 0.03	1.4 ± 0.36
DF N-Mg doped	400	62.9 ± 0.20	3.5 ± 0.04	1.6 ± 0.002	18.0 ± 1.2
DF N-Mg doped	600	72.8 ± 0.61	1.9 ± 0.02	2.2 ± 0.02	4.8 ± 0.11

Proximate analysis

Table 3 shows the volatiles, fixed carbon, ash, and moisture content of the biochars obtained from the Proximate Analysis. The ash content increased as production temperature increased, due to the accumulation of inorganic elements during the reduction of organic constituents (Enders, et al., 2012). Fixed carbon also increased with increasing temperature due to the removal of volatile matter, leaving the more stable carbon in the biomass (Yang, et al., 2020),

while the volatile matter decreased with increasing temperature, because at higher temperatures more organic compounds from the biochar are released. The ash content is significantly higher in N-Mg doped char that the than in raw biochar, a consequence of the impregnation of Mg ions in the biochar.

Table 3: Proximate analysis results from DF and PW biochar.

Dry basis	Temperature (°C)	Volatile (wt. %)	Fixed carbon (wt. %)	Ash (wt. %)	Moisture (wt. %)
WS Raw	400	22.6 ± 1.2	59.9 ± 0.43	17.4 ± 0.82	3.9 ± 0.01
WS Raw	600	16.5 ± 0.14	64.7 ± 1.4	18.7 ± 1.3	3.5 ± 0.07
WS N-doped	400	24.3 ± 0.69	55.4 ± 0.45	20.3 ± 0.25	3.8 ± 0.79
WS N-doped	600	22.4 ± 0.35	55.5 ± 0.24	22.1 ± 0.46	3.6 ± 0.25
WS N-Mg doped	400	49.2 ± 0.32	19.2 ± 0.06	31.6 ± 0.38	5.0 ± 0.48
WS N-Mg doped	600	33.9 ± 2.2	24.8 ± 1.53	41.3 ± 0.65	3.8 ± 0.63
DF Raw	400	28.1 ± 0.03	71.6 ± 0.14	0.3 ± 0.11	2.3 ± 0.04
DF Raw	600	10.3 ± 0.15	88.8 ± 0.24	0.9 ± 0.09	0.94 ± 0.001
DF N-doped	400	26.5 ± 0.47	73.0 ± 037	0.5 ± 0.10	2.4 ± 0.01
DF N-doped	600	7.8 ± 0.17	91.6 ±0.09	0.6 ± 0.26	1.2 ± 0.05
DF N-Mg doped	400	29.4 ± 0.08	57.2 ± 0.84	13.35 ± 0.93	4.8 ± 0.44
DF N-Mg doped	600	7.1 ± 0.43	74.5 ± 0.08	18.38 ± 0.51	1.7 ± 0.001

Gas physisorption analysis

Biochar samples were analyzed by CO_2 adsorption to determine the porous structure of the biochar. Figure 5 (below) shows the CO_2 adsorption isotherms for wheat straw (A) and douglas fir (B) and Figure 6 shows the pore size distribution for the same. The results of the specific surface area analysis and pore volume are provided in Table 4.

The surface area and the pore volume of all biochar samples increased as pyrolysis temperature increased for the CO_2 adsorption, due to the removal of volatile compounds which allowed

Table 4: Surface area and pore volume of the biochars.formation of micropores on the biochar surface.

Sample	Temperature (°C)	SA_{CO2} (m^2/g)	PV_{micro} (cm^3/g)
WS Raw	400	194.6 ± 0.99	0.08 ± 0.00
WS Raw	600	299.7 ± 0.11	0.12 ± 0.00
DF Raw	400	294.2 ± 2.2	0.12 ± 0.00
DF Raw	600	511.61 ± 4.3	0.20 ± 0.00
WS N-doped	400	220.9 ± 2.3	0.09 ± 0.00
WS N-doped	600	234.1 ± 3.7	0.10 ± 0.00
DF N-doped	400	314.16 ± 3.5	0.13 ± 0.00
DF N-doped	600	516.40 ± 3.2	0.21 ± 0.00
WS N-Mg doped	400	70.66 ± 1.8	0.03 ± 0.00
WS N-Mg doped	600	139.03 ± 2.5	0.06 ± 0.00
DF N-Mg doped	400	188.72 ± 1.2	0.08 ± 0.00
DF N-Mg doped	600	443.78 ± 4.1	0.18 ± 0.00

A)

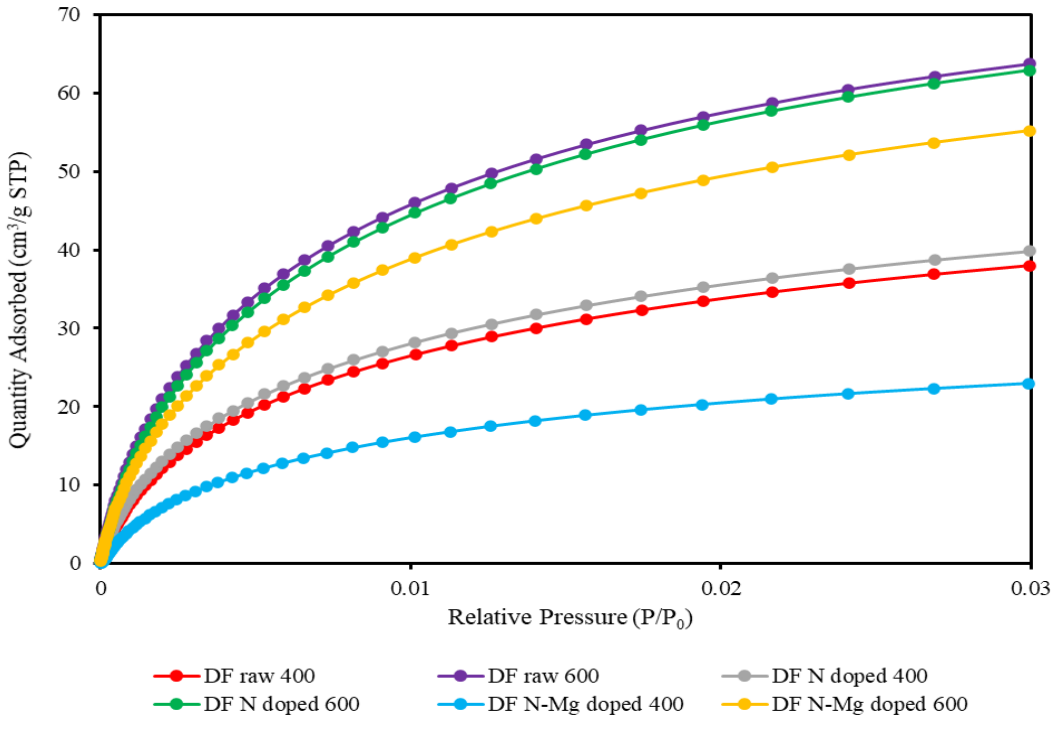

B)

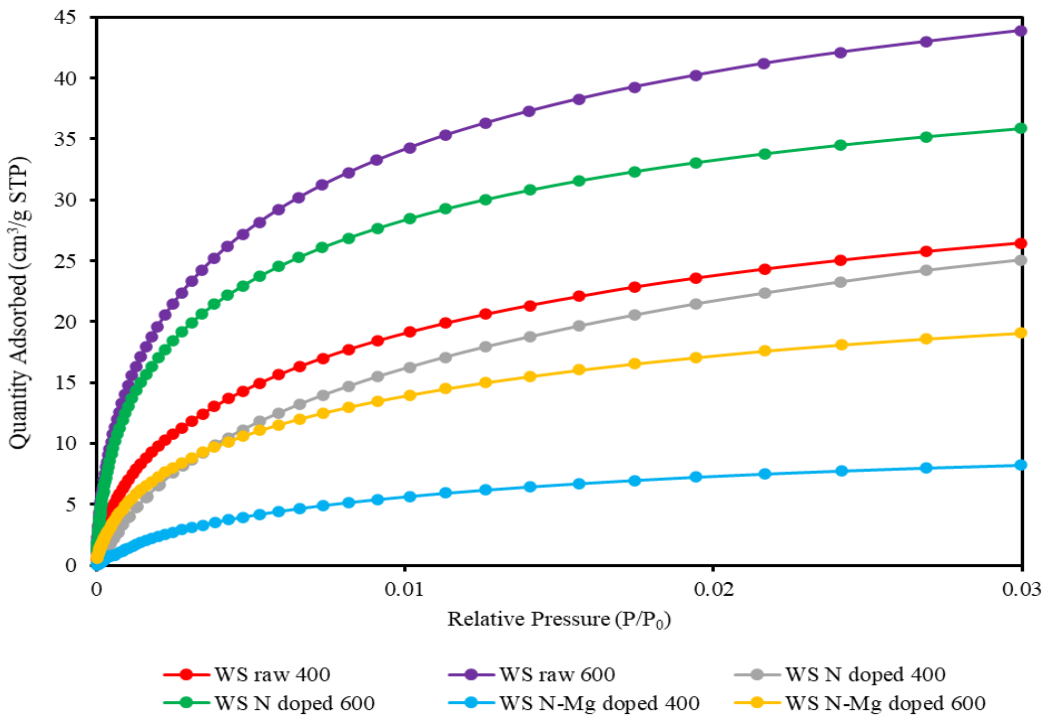

Figure 5 A: CO_2 adsorption isotherms for the WS biochars, 5 B: CO_2 adsorption isotherms for the DF biochars.

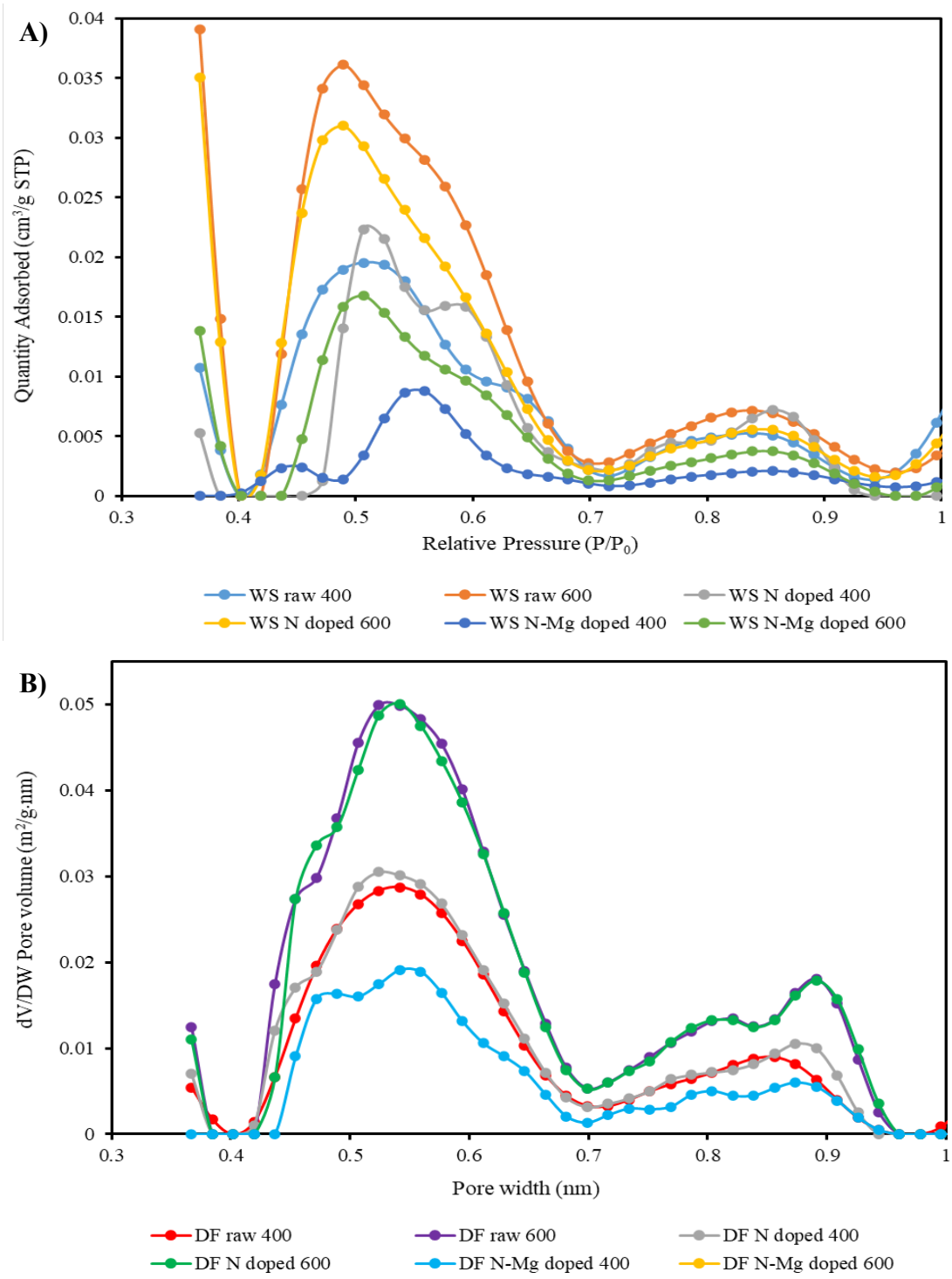

Figure 6 A: Pore size distribution for the WS biochars from CO_2 adsorption, 6 B: Pore size distribution for the DF biochars from CO_2 adsorption.

Fourier Transform Infrared Spectroscopy (FTIR)

The FTIR spectra are given in Figure 7 for all biochar produced at 400 and 600 °C. This analysis was performed to determine the functional groups present in the majority of the biochar samples. Results are as follows:

- The hydrogen-bonded stretching O-H band appeared as a broad peak at 3400 cm^{-1}.
- The C-H stretching asymmetric band formed around 2926 cm^{-1}, and is associated with the aliphatic functional group methylene (-CH_2-).
- C-H bending was identified at approximately the band near 1375 cm^{-1} for methyl groups.
- The C≡C functional group for terminal alkyne was found at about 2150 cm^{-1}.
- C=C ring stretch absorptions occurred about 1600 cm^{-1}.
- C-O stretching vibration for alcohol usually occurs in the range 1260–1000 cm^{-1}. This band can represent primary, secondary, or tertiary structure to an alcohol.
- N-H bending vibration showed between 1640–1550 cm^{-1} for primary and secondary amides.
- C-N stretch for amines occurred in the range of 1350–1000 cm^{-1}.

The FTIR results suggest the biochar samples have many important O and N containing functional groups, some of which may play an important role on the removal of odorous materials released by composting facilities.

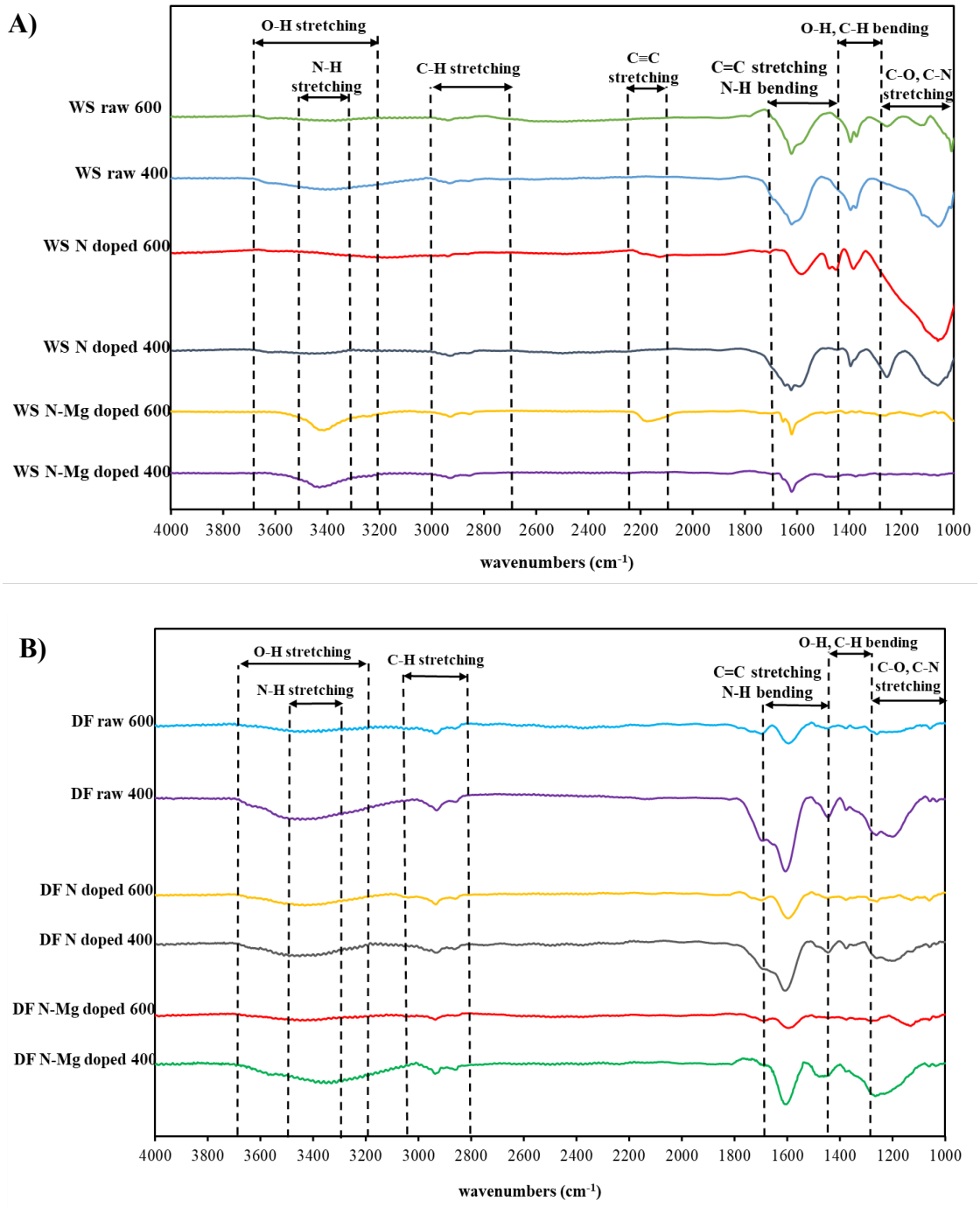

Figure 7 A: Fourier-transform infrared spectra (FTIR) of the WS biochar sample, 7 B: Fourier-transform infrared spectra (FTIR) of the DF biochar sample.

pH analysis

Figure 8 shows the values of pH of the biochar samples. The pH of all biochar samples in water increased from 6.73 to 11.54 with the increase in pyrolysis temperature. Based on the pH values obtained, all the char were alkaline, except for the DF raw biochar (6.73), where the low ash content reduces the alkalinity.

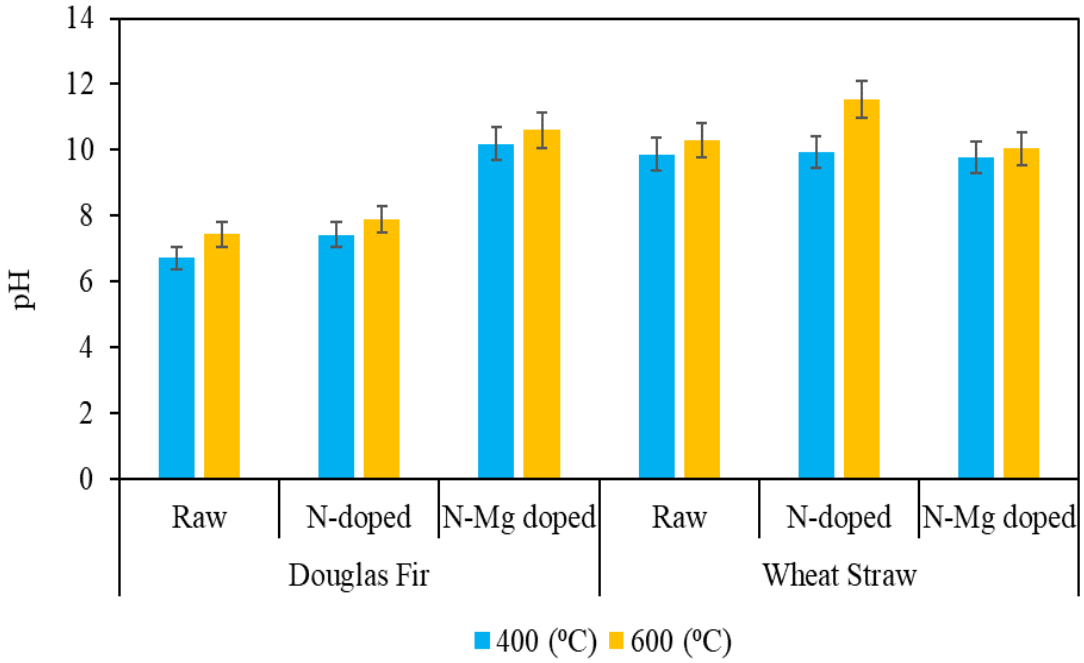

Figure 8: pH of the biochar samples at 400 and 600 C.

Adsorption studies

H_2S adsorption studies

The breakthrough curves from the different chars are presented in Figure 9. The breakthrough time was defined as the time when the first non-zero H_2S concentration was measure in the column exit. WS raw 600, WS N doped 600, WS raw 400, and DF N doped 600 biochars showed the longest breakthrough time with 160, 150, 140 and 50 minutes, respectively. Some of the char characteristics that have an important role in the adsorption of H_2S are the presence of ash, surface area, pH, pore size and surface chemistry (Ayiania, et al., 2019).

The DF N-doped 600 biochar showed the highest surface area (SA_{CO2}=516.40 m^2/g), which indicates a greater number of adsorption sites and space are available for H_2S adsorption; this factor influenced the adsorption capacity of H_2S for this biochar.

The pH values for the biochars with higher breakthrough time ranged from 7.91 to 11.54. The alkalinity of the char can be attributed to the high inorganic fraction and also to the nitrogen

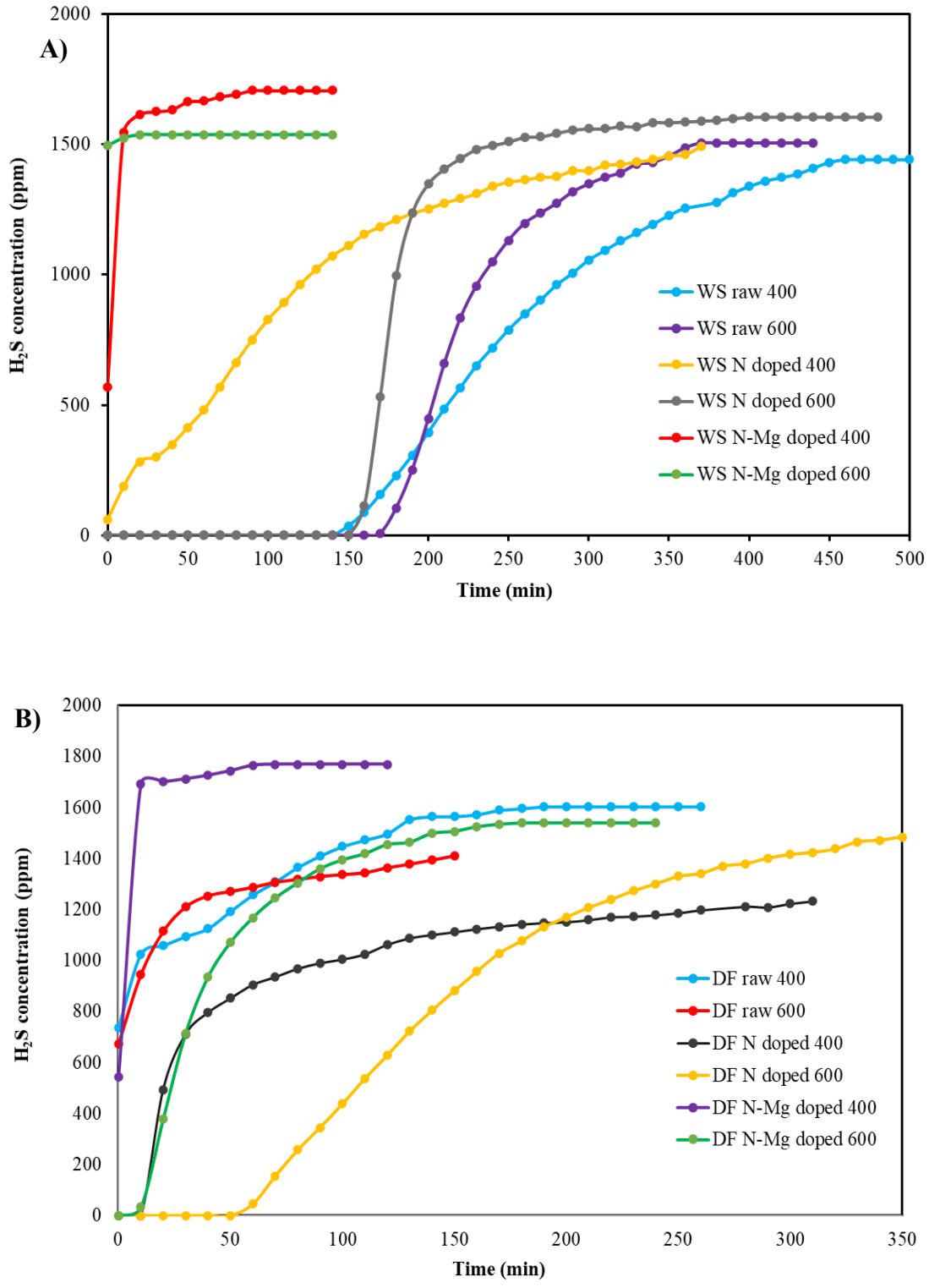

Figure 9 A: Typical breakthrough curves of H_2S adsorption on WS biochars, 9 B: Typical breakthrough curves of H_2S adsorption on DF biochars.

content. A pH in the basic range promotes the dissociation of H_2S and has a positive influence in H_2S adsorption (Bagreev et al., 2001).

The moisture content of biochar also facilitates the dissociation of H_2S, which can be oxidized to sulfur and sulfur dioxide (Yan, et al., 2002). The moisture fraction of the biochar samples varied from 0.94 to 4.8 w.%. Bagreev and Bandosz (2004) and Adib et al (2000) suggest that the moisture content contributes to H_2S adsorption, and propose that H_2S diffuses into the water film on the surface of carbon, causing a further reaction with adsorbed oxygen, which forms oxidized species of sulfur. The H_2S adsorption capacity of the best performing biochar (WS raw 600) is 27.7 mg/g. This value is comparable with the H_2S adsorption capacity of a biochar derived from anaerobic digestion fiber (21-51 mg H_2S/g char) (Ayiania, et al., 2019). The emission of volatile surfur compounds (VSCs) (e.g., methyl disulfide, methyl sulfide, carbon disulfide, methyl mercaptan, and H_2S) in composting units has been reported to be close to 0.561 mg H_2S/g waste (Han, et al., 2018). To remove such quantities of VSCs, a biochar with capacity to remove 27.7 mg H_2S/g is needed, and will be required in a ratio of 0.020 g biochar/g waste (or 2% weight of biochar).

NH_3 adsorption studies

The breakthrough curves from the different chars are presented in Figure 10. WS N-Mg doped 400, DF raw 400, WS N-Mg doped 600, and DF N doped 400 biochars showed the longest breakthrough time with 190, 90, 80 and 60 minutes, respectively. Based on the statistic correlation analysis, the most important factor in the adsorption of NH_3 was the oxygen content, suggesting that the acidic functional groups present on biochar surface are the governing characteristic in the increase of adsorption of NH_3, due to the basic nature of this gas.

Huang et al (2008) and Asada et al (2006) reported that NH_3 adsorption capacity has a linear relationship with the acidic functional groups present on the biochar. The results obtained in this research are consistent with those found by Mochizuki et al (2016) which indicate that the adsorption capacity of NH_3 was affected by the Van der Waals interaction and the bonding between the acidic functional groups present on the char surface and NH_3 molecules. The NH_3 adsorption capacity of the best biochar produced (DF raw 400) was 0.47 mg/g. This value is comparable with the NH_3 adsorption capacity of a non activated biochar reported in the literature and is very low (0.15-5.09 mg NH_3/g char)-- activation of biochars with phosphoric acid greatly increased ammonia adsorption (24-53 mg NH_3/g biochar) (Ro, et al., 2005).

The emission of NH_3 in composting facilities reported in the literature is between 0.018 and 1.150 mg/g of waste (Clemens & Cuhls, 2003; Cadena, et al., 2009). This means that for a material releasing 0.35 mg NH_3/g of waste and a biochar with a capacity to remove 40 mg NH_3/g biochar (produced with phosphoric acid), all NH_3 released can be adsorbed by adding 0.00875 g char/g waste. In the case of a non activated biochar with low adsorption capacity (0.47 mg NH_3/g biochar), 0.744 g of char per g of waste will be needed.

This amount of biochar is not practical to use in composting, and clearly shows the importance of continuing to develop engineered materials with a high capacity to adsorb NH_3.

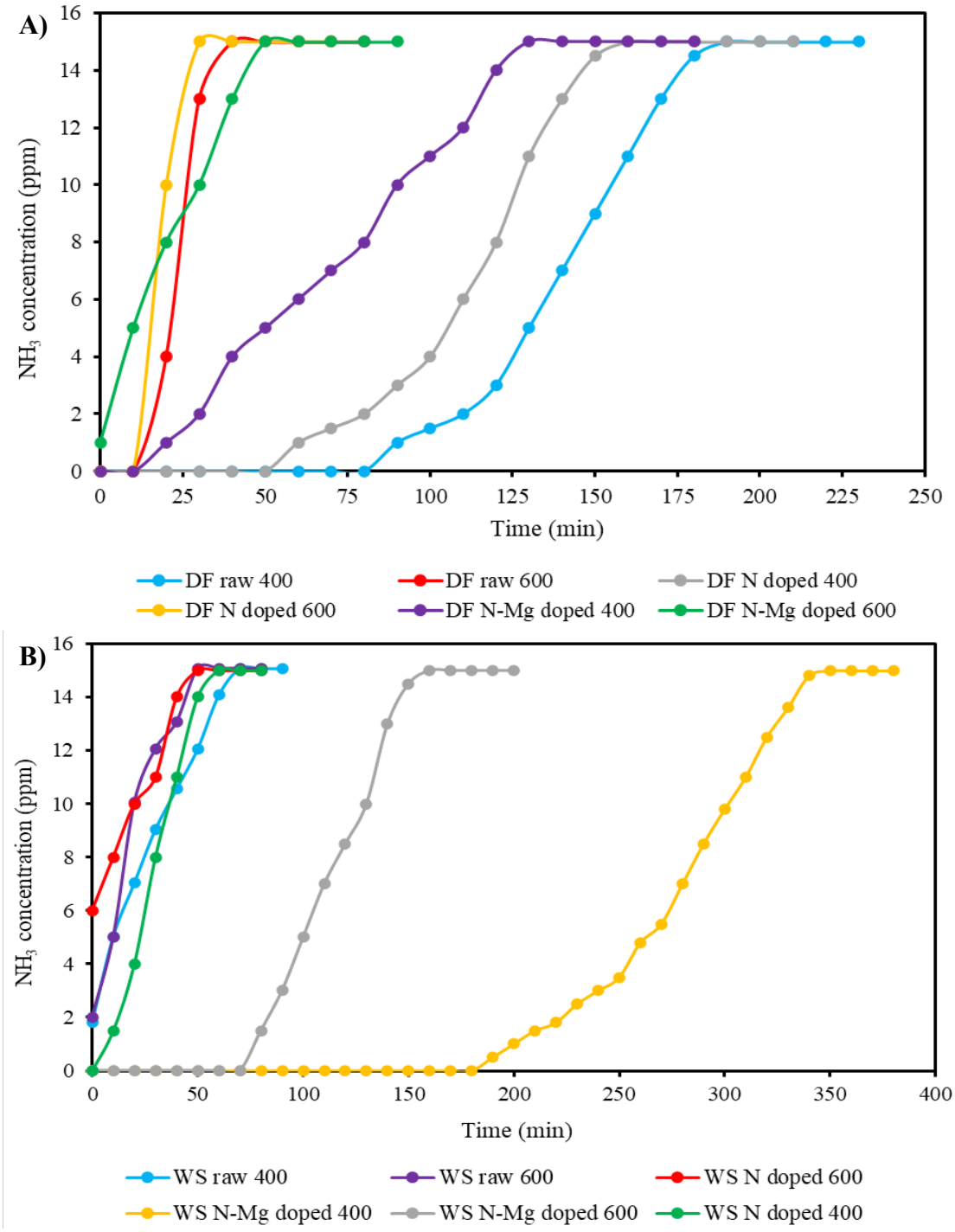

Figure 10 A: Typical breakthrough curves of NH_3 adsorption on WS biochars, 10 B: Typical breakthrough curves of NH_3 adsorption on DF biochars.

CO_2 adsorption studies

Figure 11 shows the biochar adsorption isotherms for the CO_2 adsorption analysis. The adsorption study results show that all biochar samples adsorbed CO_2. Those with the longest breakthrough time were WS N doped 600, WS raw 400, DF raw 600 and WS raw 600, with 120, 100, 80 and 70 minutes, respectively. Based on the correlation analysis it was determined that the pH, ash and nitrogen content are the most influential factors in the CO_2 adsorption process, as all factors contribute to making the biochar more alkaline, which better adsorbs CO_2.

Alkaline metals within the char are attracted to CO_2 (due to its acidic nature): basic species make the carbon surface more basic, increasing the CO_2 adsorption capacity. The introduction of nitrogen groups to the surface of the biochar increases the basicity of biochar, and makes more adsorption sites available for CO_2 adsorption (Zhang, et al., 2010; Caglayan & Aksoylu, 2013; Somy, et al., 2009; Plaza, et al., 2007). The CO_2 adsorption capacity of the highest performing biochar produced (WS raw 400) is 0.49 mg/g. This value is very low compared with CO_2 adsorption of biochar reported in the literature: 57-176 mg CO_2/g char (Li & Xiao, 2019). The emission of CO_2 in composting facilities has been reported to be 150-370 mg/g waste (Komilis & Ham, 2006). This means that to remove 200 mg CO_2/g waste, with a biochar with the capacity to remove 57-176 mg CO_2/g biochar, more than 1g char/g waste will be needed.

Because of the high amount of CO_2 produced by composting, it is very unlikely to a biochar could be developed with sufficient adsorption capacity to remove all the CO_2 released in the facility at an economically viable rate. However, in the course of utilizing biochar to treat other emissions, adsorption of some CO_2 may lead incidentally to the capture of some portion of the CO_2 that would otherwise be lost, benefitting carbon sequestration.

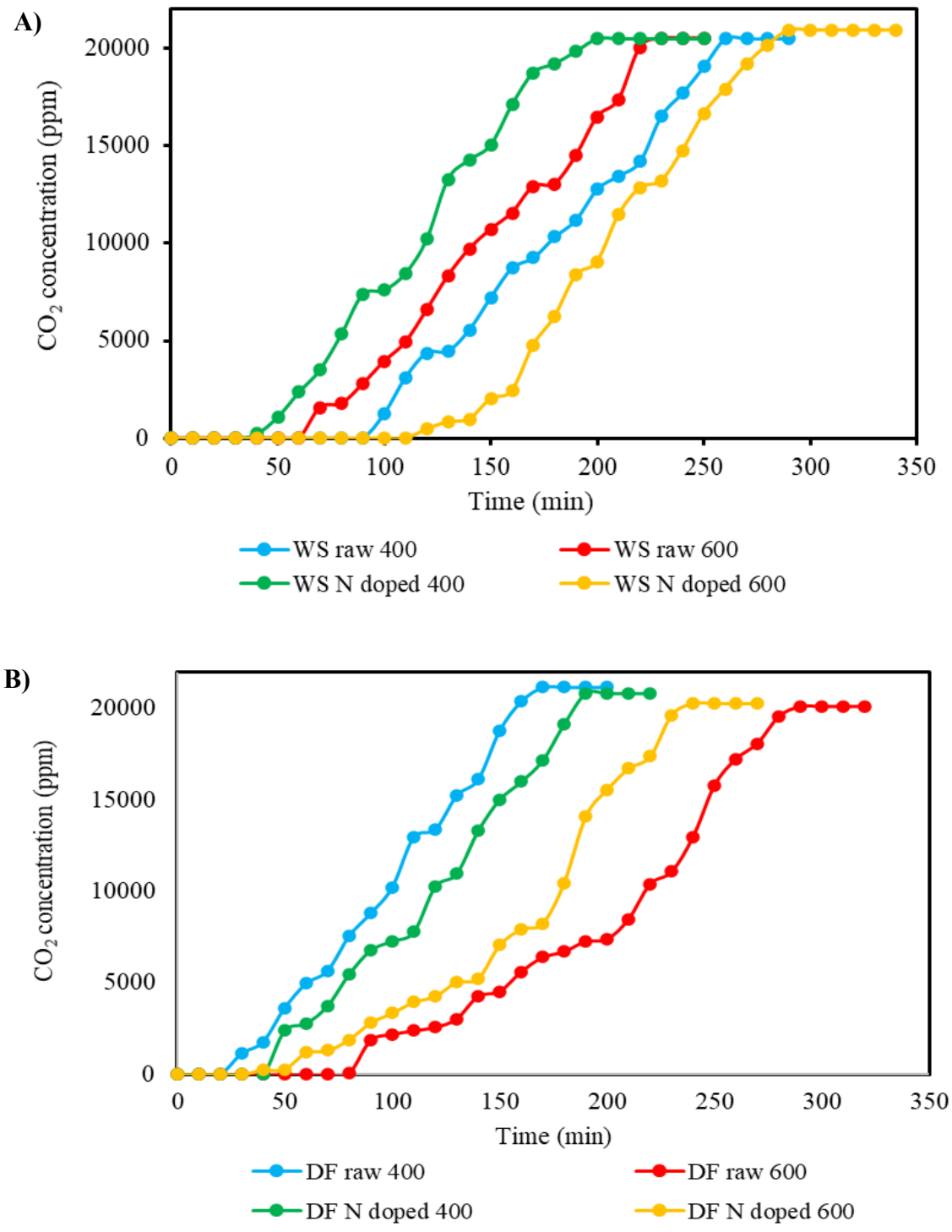

Figure 11 A: Typical breakthrough curves of CO_2 adsorption on WS biochars, 11 B: Typical breakthrough curves of CO_2 adsorption on DF biochars.

Formulation of Engineered Biochar Cocktails for Odor Emission/VOC Removal in Compost Facilities

Table 5 shows a range of estimated emissions factors from compost for five common compounds as described in the literature. It also shows a range of adsorption capacities of engineered biochars for those same contaminants, including those reported on in this study (H_2S, NH_3, CO_2), also as described in the literature. The amount of biochar needed to treat the emissions is also calculated. Based on the target compounds for which treatment is desired, a biochar cocktail (a blend of engineered biochar samples) could be developed to treat a suite of contaminants.

Table 5: Amount of biochar needed to treat each contaminant.

Target Compound	Emission factor (mg/g waste)	References	Adsorption capacity of the biochar in the literature (mg/ g char)	References	Amount of biochar to treat the contaminats (g char/g waste)
H_2S	0.561	(Han, et al., 2018)	21-51	(Ayiania, et al. 2019)	0.011- 0.027
NH_3	0.018 - 1.150	(Clemens & Cuhls, 2003; Cadena, et al. 2009)	24-53	(Ro, et al., 2005)	0.00034-0.048
CO_2	150-370	(Komilis & Ham, 2006)	57-176	(Li & Xiao 2019)	0.85-6.5
CH_4	0.05-0.49	(Amlinger, et al., 2008)	6.5	(Song, et al., 2021)	0.0076-0.075
N_2O	0.074-1.57	(Zheng, et al., 2020)	300	(Cha & Kong, 1995)	0.00024 - 0.0052

The results shown in Table 5 suggest that for compounds other than carbon dioxide, there are strategies reported in the literature that could be used to produce chars with capacities sufficiently high to justify their use in composting facilities at concentrations below 7% by weight. For several of the compounds described here (H_2S, NH_3 and N_2O), the amount needed is much less, roughly 2% or less by weight. However, in our laboratory experiments we were not able to obtain biochars with adsorption capacity sufficiently high to be economically used in composting facilities. Our results for H_2S indicate an adsorption capacity in the range of those values from the literature, but our results for NH_3 and CO_2 were lower than those found in other studies. In this work we studied a number of standard activation strategies with two feedstocks, but observed poor adsorption results for CO_2 and NH_3. In the future we will need to explore other activation strategies reported in the literature, using feedstocks available in the Pacific Northwest.

The removal of CO_2 with biochar is unlikely to be economically viable due to the high quantities of CO_2 released during composting, which necessitates an impractically large amount of biochar for adsorption. Because the results found elsewhere (see Table 5) indicate potential higher adsorption capability, a biochar cocktail is still a promising concept. However, more research is needed on feedstocks available in Washington State to produce chars with high adsorption capacities.

Conclusions

The results of this project show that biochar produced from the same feedstock, pyrolyzed at different temperatures (400 and 600°C) and either raw, N doped, or Mg-N doped, have different capacities to adsorb H_2S, NH_3 and CO_2.

- The thermogravimetric analysis results show a significant amount of ash in WS, an important property which contributes to high levels of H_2S retention as it helps to increase the pH of the biochar.
- Surface area is another important metric which enhances gas adsorption. The biochar produced in this project are mostly dominated by micropores. Biochar produced at 600°C showed a higher surface area compared to those produced that 400°C.
- Nitrogen content, which has been previously found to modify the electronic structure of biochar, has a significant influence on the removal of H_2S and CO_2. Biochar pyrolized at 600°C has more nitrogen functional groups, which makes the biochar more alkaline, contributing to the adsorption of acidic pollutants such as CO_2.
- The FTIR analysis showed the presence of oxygen functional groups on the majority of the biochar samples. This element (oxygen) is a the main factor supporting NH_3 adsorption.
- A X-ray photoelectron spectroscopy (XPS) analysis is recommended to determine the elemental composition of the biochar surface with greater certainty.

The adsorption capacities obtained in this project are still below those reported in the literature. The results suggests that although biochar with adsorption capacity sufficiently high to be economically used in composting facilities were not produced, there are strategies reported in the literature to produce biochar with sufficiently high capacity to justify their use in composting facilities at concentrations below 10% by weight. These strategies need to be further explored with feedstocks available in Washington State to produce biochar with high adsorption capacities.

This is a complex problem that warrants further research. While this project examined engineered biochar cocktails to address three common pollutants (H_2S, NH_3, CO_2) there is a wide range of emissions, including VOCs, that will require further research and development of targeted biochar cocktails. This research demonstrates the efficacy of biochar as a means to address noxious gases and illustrates the potential for engineered biochar cocktails.

References

Adib, F., Bagreev, A. & Bandosz, T. J., 2000. Adsorption/Oxidation of Hydrogen Sulfide on Nitrogen-Containing Activated Carbons. *Langmuir,* Volume 16, pp. 1980-1986.

Amlinger, F., Peyr, S. & Cuhls, C., 2008. Green house gas emissions from composting and mechanical biological treatment. *Waste management & research,* p. 47–60.

Asada, T., Ohkubo, T., Kawata, K. & Oikawa, K., 2006. Ammonia adsorption on bamboo charcoal with acid treatment. *Journal of Health Science,* Volume 52, pp. 585-589.

Ayiania, M. et al., 2019. Production and characterization of H2S and PO43− carbonaceous adsorbents from anaerobic digested fibers. *Biomass and Bioenergy,* Volume 120, pp. 339-349.

Ayiania, M. et al., 2020. Deconvoluting the XPS spectra for nitrogen-doped chars: An analysis from first principles. *Carbon,* Volume 162, pp. 528-544.

Bagreev, A., et al., 2001. pH of activated carbon surface as an indication of its suitability for H2S removal from moist air streams. *Carbon,* Volume 39, pp. 1897-1905.

Bagreev, A. & Bandosz, T., 2004. Carbonaceous materials for gas phase desulfurization: Role of surface heterogeneity. *Preprints of Papers - American Chemical Society, Division of Fuel Chemistry,* Volume 49, pp. 817-821.

Cadena, E. et al., 2009. A methodology to determine gaseous emissions in a composting plant. *Waste Management,* Volume 29, pp. 2799-2807.

Caglayan, B. S. & Aksoylu, A. E., 2013. CO2 adsorption on chemically modified activated carbon. *Journal of Hazardous Materials,* Volume 252–253, pp. 19-28.

Cantrell, K. B. et al., 2012. Impact of pyrolysis temperature and manure source on physicochemical characteristics of biochar. *Bioresource Technology,* Volume 107, pp. 419-428.

Cha, C. Y. & Kong, Y., 1995. Enhancement of NOx adsorption capacity and rate of char by microwaves. *Carbon,* Volume 33, pp. 1141-1146.

Clemens, J. & Cuhls, C., 2003. Greenhouse gas emissions from mechaniscal and biological waste treatment of municipal waste. *Environmental Technology,* Volume 24, pp. 745-754.

Crombie, K. et al., 2013. The effect of pyrolysis conditions on biochar stability as determined by three methods. *GCB Bioenergy,* Volume 5, pp. 122-131.

Dhamodharan, K., et al., 2019. Emission of volatile organic compounds from composting: A review on assessment, treatment and perspectives. *Science of The Total Environment,* p. 133725.

Ecology, 2019. Compost. https://ecology.wa.gov/Waste-Toxics/Reducing-recyclingwaste/Organic-materials/Managing-organics-compost Retrieved June 2021.

Eitzer, B. D., 1995. Emissions of Volatile Organic Chemicals from Municipal Solid Waste Composting Facilities. *Environmental Science & Technology ,* Volume 29, pp. 896-902.

Enders, A. et al., 2012. Characterization of biochars to evaluate recalcitrance and agronomic performance. *Bioresource Technology,* Volume 114, pp. 644-653.

Font, X., Artola, A. & Sánchez, A., 2011. Detection, Composition and Treatment of Volatile Organic Compounds from Waste Treatment Plants. *Sensors (Basel, Switzerland),* Volume 11, p. 4043–4059.

Han, Z. et al., 2018. Emission characteristics of volatile sulfur compounds (VSCs) from a municipal sewage sludge aerobic composting plant. *Waste Management,* Volume 77, pp. 593-602.

Huang, C.-C., Li, H.-S. & Chen, C.-H., 2008. Effect of surface acidic oxides of activated carbon on adsorption of ammonia. *Journal of Hazardous Materials,* Volume 159, pp. 523-527.

Komilis, D. & Ham, R., 2006. Carbon dioxide and ammonia emissions during composting of mixed paper, yard waste and food waste. *Waste Manag,* Volume 26, pp. 62-70.

Komilis, D. P., Ham, R. K. & Park, J. K., 2004. Emission of volatile organic compounds during composting of municipal solid wastes. *Water Research,* pp. 1707-1714.

Lehmann, J. & Joseph, S., 2015. *Biochar for Environmental Management : Science, Technology and Implementation.* Second Edition ed. London, UNITED KINGDOM: Taylor & Francis Group.

Li M, Xiao R, 2019. Preparation of a dual Pore Structure Activated Carbon from Rice Husk Char as an Adsorbent for CO2 Capture. Fuel Processing Technology, Vol 186: 35-39

Ma, J., Wilson, K., Zhao, Q., Yorgey, G., Frear, C., 2013. Odor in Commercial Scale Compost: Literature Review and Critical Analysis, Washington State Department of Ecology.

Mochizuki, T., Kubota, M., Matsuda, H. & Camacho, L. F. D., 2016. Adsorption behaviors of ammonia and hydrogen sulfide on activated carbon prepared from petroleum coke by KOH chemical activation. *Fuel Processing Technology,* Volume 144, pp. 164-169.

Plaza, M. et al., 2007. CO2 capture by adsorption with nitrogen enriched carbons. *Fuel,* Volume 86, pp. 2204-2212.

Rodrigues, C. C., Moraes, D. d., Nóbrega, S. W. d. & Barboza, M. G., 2007. Ammonia adsorption in a fixed bed of activated carbon. *Bioresource Technology,* Volume 98, pp. 886-891.

Ro, K. S. et al., 2005. Removing Gaseous NH3 Using Biochar as an Adsorbent. *Agriculture,* Volume 5, pp. 991-1002.

Sánchez-Monedero, M., Sánchez-García, M., Alburquerque, J. & Cayuela, M., 2019. Biochar reduces volatile organic compounds generated during chicken manure composting. *Bioresource Technology,* Volume 288, p. 121584.

Somy, A. et al., 2009. Adsorption of carbon dioxide using impregnated activated carbon promoted by Zinc. *International Journal of Greenhouse Gas Control,* Volume 3, pp. 249-254.

Song, Y., Zhou, X. & Wang, J. A., 2021. Adsorption performance of activated carbon for methane with low concentration at atmospheric pressure. *Energy Sources, Part A: Recovery, Utilization, and Environmental Effects,* Volume 43, pp. 1337-1347.

Suliman, W. et al., 2016a. Influence of feedstock source and pyrolysis temperature on biochar bulk and surface properties. *Biomass and Bioenergy,* Volume 84, pp. 37-48.

Suliman, W. et al., 2016b. Modification of biochar surface by air oxidation: Role of pyrolysis temperature. *Biomass and Bioenergy,* Volume 85, pp. 1-11.

Swati, A. & Hait, S., 2018. Greenhouse Gas Emission During Composting and Vermicomposting of Organic Wastes – A Review. *Clean – Soil, Air, Water.*

Wang, T., Camps-Arbestain, M., Hedley, M. & Bishop, P., 2012. Predicting phosphorus bioavailability from high-ash biochars. *Plant and Soil,* Volume 357, pp. 173-187.

Yang, X. et al., 2020. Effects of carbonization conditions on the yield and fixed carbon content of biochar from pruned apple tree branches. *Renewable Energy,* Volume 146, pp. 1691-1699.

Yang, Z., Miao, H., Rui, Z. & Ji, H., 2019. Enhanced Formaldehyde Removal from Air Using Fully Biodegradable Chitosan Grafted β-Cyclodextrin Adsorbent with Weak Chemical Interaction. *Polymers,* Volume 11.

Yan, R., Liang, D. T., Tsen, L. & Tay, J. H., 2002. Kinetics and Mechanisms of H2S Adsorption by Alkaline Activated Carbon. *Environ. Sci. Technol.,* Volume 36, pp. 4460-4466.

Zhang, L. et al., 2018. Catalytic Pyrolysis of Biomass and Polymer Wastes. *Catalysts,* 8(12), p. 659.

Zhang, Z., Xu, M., Wang, H. & Li, Z., 2010. Enhancement of CO2 adsorption on high surface area activated carbon modified by N2, H2 and ammonia. *Chemical Engineering Journal,* Volume 60, pp. 571-577.

Zheng, J. et al., 2020. N2O emission factors of full-scale animal manure windrow composting in cold and warm seasons. *Bioresource Technology,* p. 123905.

Appendix A

The correlation analysis for the different adsorption experiments is presented in the tables and figures below.

Table A1: Correlation analysis for the DF raw biochar for the H_2S adsorption test.

Row	Temp	SACO2	pH	Ash	M (wt. %)	N (wt. %)	BRK_T (min)
Temp	1	1	1	1	-1	1	0
SACO2	1	1	1	1	-1	1	0
pH	1	1	1	1	-1	1	0
Ash	1	1	1	1	-1	1	0
M (wt. %)	-1	-1	-1	-1	1	-1	0
N (wt. %)	1	1	1	1	-1	1	0
BRK_T (min)	0	0	0	0	0	0	1

Table A2: Correlation analysis for the DF N doped biochar for the H_2S adsorption test.

Row	Temp	SA_{CO2}	pH	Ash	M (wt. %)	N (wt. %)	BRK_T (min)
Temp	1	1	1	1	-1	1	1
SACO2	1	1	1	1	-1	1	1
pH	1	1	1	1	-1	1	1
Ash	1	1	1	1	-1	1	1
M (wt. %)	-1	-1	-1	-1	1	-1	-1
N (wt. %)	1	1	1	1	-1	1	1
BRK_T (min)	1	1	1	1	-1	1	1

Table A3: Correlation analysis for the DF Mg-N doped biochar for the H_2S adsorption test.

Row	Temp	SACO2	pH	Ash	M (wt. %)	N (wt. %)	BRK_T (min)
Temp	1	1	1	1	-1	1	1
SACO2	1	1	1	1	-1	1	1
pH	1	1	1	1	-1	1	1
Ash	1	1	1	1	-1	1	1
M (wt. %)	-1	-1	-1	-1	1	-1	-1
N (wt. %)	1	1	1	1	-1	1	1
BRK_T (min)	1	1	1	1	-1	1	1

Table A4: Correlation analysis for the WS raw biochar for the H_2S adsorption test.

Row	Temp	SACO2	pH	Ash	M (wt. %)	N (wt. %)	BRK_T (min)
Temp	1	1	1	1	-1	1	1
SACO2	1	1	1	1	-1	1	1
pH	1	1	1	1	-1	1	1
Ash	1	1	1	1	-1	1	1
M (wt. %)	-1	-1	-1	-1	1	-1	-1
N (wt. %)	1	1	1	1	-1	1	1
BRK_T (min)	1	1	1	1	-1	1	1

Table A5: Correlation analysis for the WS N doped biochar for the H_2S adsorption test.

Row	Temp	SACO2	pH	Ash	M (wt. %)	N (wt. %)	BRK_T (min)
Temp	1	1	1	1	-1	1	1
SACO2	1	1	1	1	-1	1	1
pH	1	1	1	1	-1	1	1
Ash	1	1	1	1	-1	1	1
M (wt. %)	-1	-1	-1	-1	1	-1	-1
N (wt. %)	1	1	1	1	-1	1	1
BRK_T (min)	1	1	1	1	-1	1	1

Table A6: Correlation analysis for the WS Mg-N doped biochar for the H_2S adsorption test.

Row	Temp	SACO2	pH	Ash	M (wt. %)	N (wt. %)	BRK_T (min)
Temp	1	1	1	1	-1	1	0
SACO2	1	1	1	1	-1	1	0
pH	1	1	1	1	-1	1	0
Ash	1	1	1	1	-1	1	0
M (wt. %)	-1	-1	-1	-1	1	-1	0
N (wt. %)	1	1	1	1	-1	1	0
BRK_T (min)	0	0	0	0	0	0	1

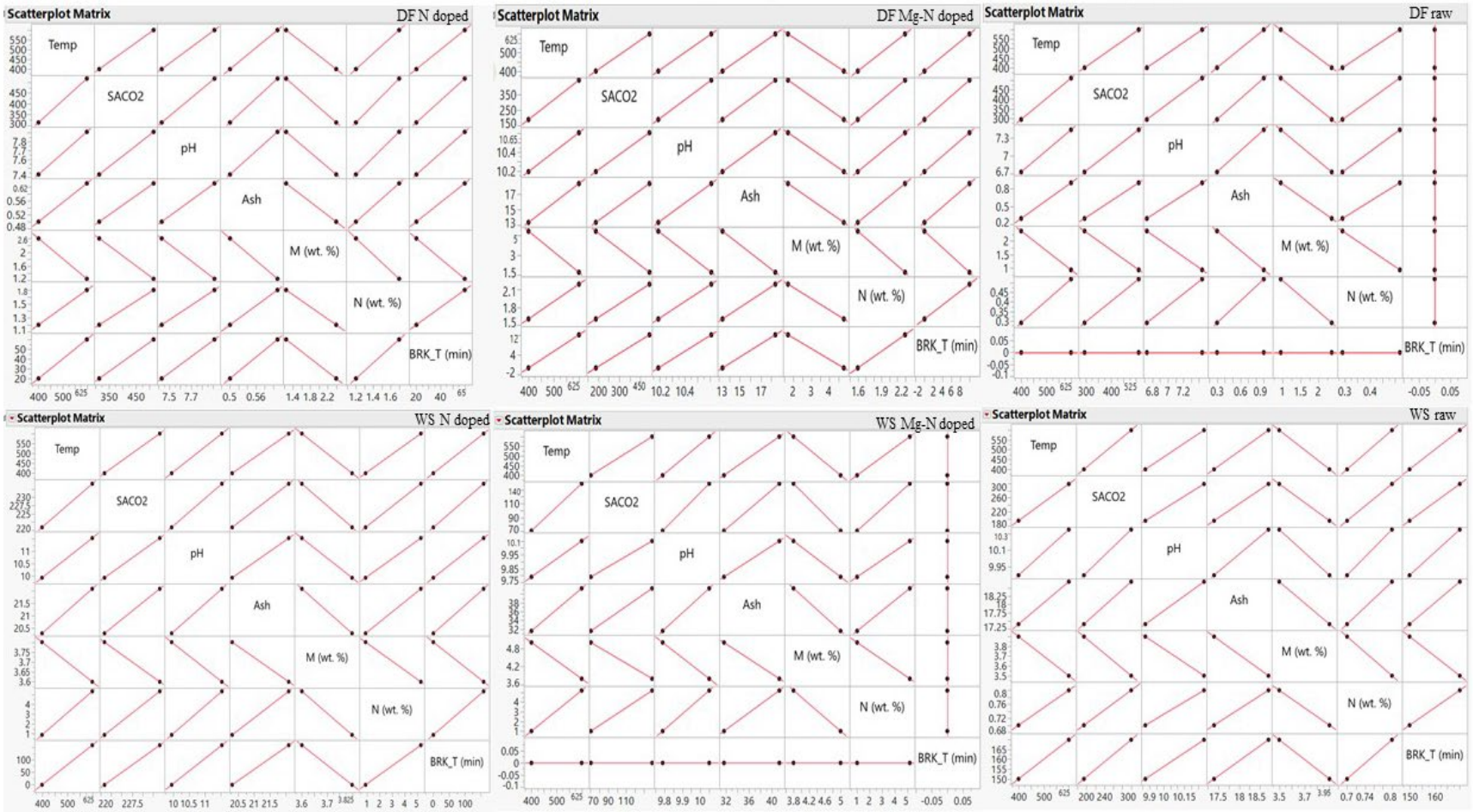

Figure A1: Scatter Plot for the correlation analysis for the H_2S adsorption experiments.

Table A7: Correlation analysis for the DF raw biochar for the NH_3 adsorption test.

Row	Temp	SACO2	pH	Ash	O (wt. %)	N (wt. %)	BRK_T (min)
Temp	1	1	1	1	-1	1	-1
SACO2	1	1	1	1	-1	1	-1
pH	1	1	1	1	-1	1	-1
Ash	1	1	1	1	-1	1	-1
O (wt. %)	-1	-1	-1	-1	1	-1	1
N (wt. %)	1	1	1	1	-1	1	-1
BRK_T (min)	-1	-1	-1	-1	1	-1	1

Table A8: Correlation analysis for the DF N doped biochar for the NH_3 adsorption test.

Row	Temp	SACO2	pH	Ash	O (wt. %)	N (wt. %)	BRK_T (min)
Temp	1	1	1	1	-1	1	-1
SACO2	1	1	1	1	-1	1	-1
pH	1	1	1	1	-1	1	-1
Ash	1	1	1	1	-1	1	-1
O (wt. %)	-1	-1	-1	-1	1	-1	1
N (wt. %)	1	1	1	1	-1	1	-1
BRK_T (min)	-1	-1	-1	-1	1	-1	1

Table A9: Correlation analysis for the DF Mg- N doped biochar for the NH_3 adsorption test.

Row	*Temp*	*SACO2*	*pH*	*Ash*	*O (wt. %)*	N (wt. %)	BRK_T (min)
Temp	1	1	1	1	-1	1	-1
SACO2	1	1	1	1	-1	*1*	-1
pH	1	1	1	1	-1	1	-1
Ash	1	1	1	1	-1	1	-1
O (wt. %)	-1	-1	-1	-1	1	-1	1
N (wt. %)	1	1	1	1	-1	1	-1
BRK_T (min)	-1	-1	-1	-1	1	-1	1

Table A10: Correlation analysis for the WS raw biochar for the NH_3 adsorption test.

Row	Temp	SACO2	pH	Ash	O (wt. %)	N (wt. %)	BRK_T (min)
Temp	1	1	1	1	-1	1	0
SACO2	1	1	1	1	-1	1	0
pH	1	1	1	1	-1	1	0
Ash	1	1	1	1	-1	1	0
O (wt. %)	-1	-1	-1	-1	1	-1	0
N (wt. %)	1	1	1	1	-1	1	0
BRK_T (min)	0	0	0	0	0	0	1

Table A11: Correlation analysis for the WS N doped biochar for the NH_3 adsorption test.

Row	Temp	SACO2	pH	Ash	O (wt. %)	N (wt. %)	BRK_T (min)
Temp	1	1	1	1	-1	1	-1
SACO2	1	1	1	1	-1	1	-1
pH	1	1	1	1	-1	1	-1
Ash	1	1	1	1	-1	1	-1
O (wt. %)	-1	-1	-1	-1	1	-1	1
N (wt. %)	1	1	1	1	-1	1	-1
BRK_T (min)	-1	-1	-1	-1	1	-1	1

Table A12: Correlation analysis for the WS Mg-N doped biochar for the NH_3 adsorption test.

Row	Temp	SACO2	pH	Ash	O (wt. %)	N (wt. %)	BRK_T (min)
Temp	1	1	1	1	-1	1	-1
SACO2	1	1	1	1	-1	1	-1
pH	1	1	1	1	-1	1	-1
Ash	1	1	1	1	-1	1	-1
O (wt. %)	-1	-1	-1	-1	1	-1	1
N (wt. %)	1	1	1	1	-1	1	-1
BRK_T (min)	-1	-1	-1	-1	1	-1	1

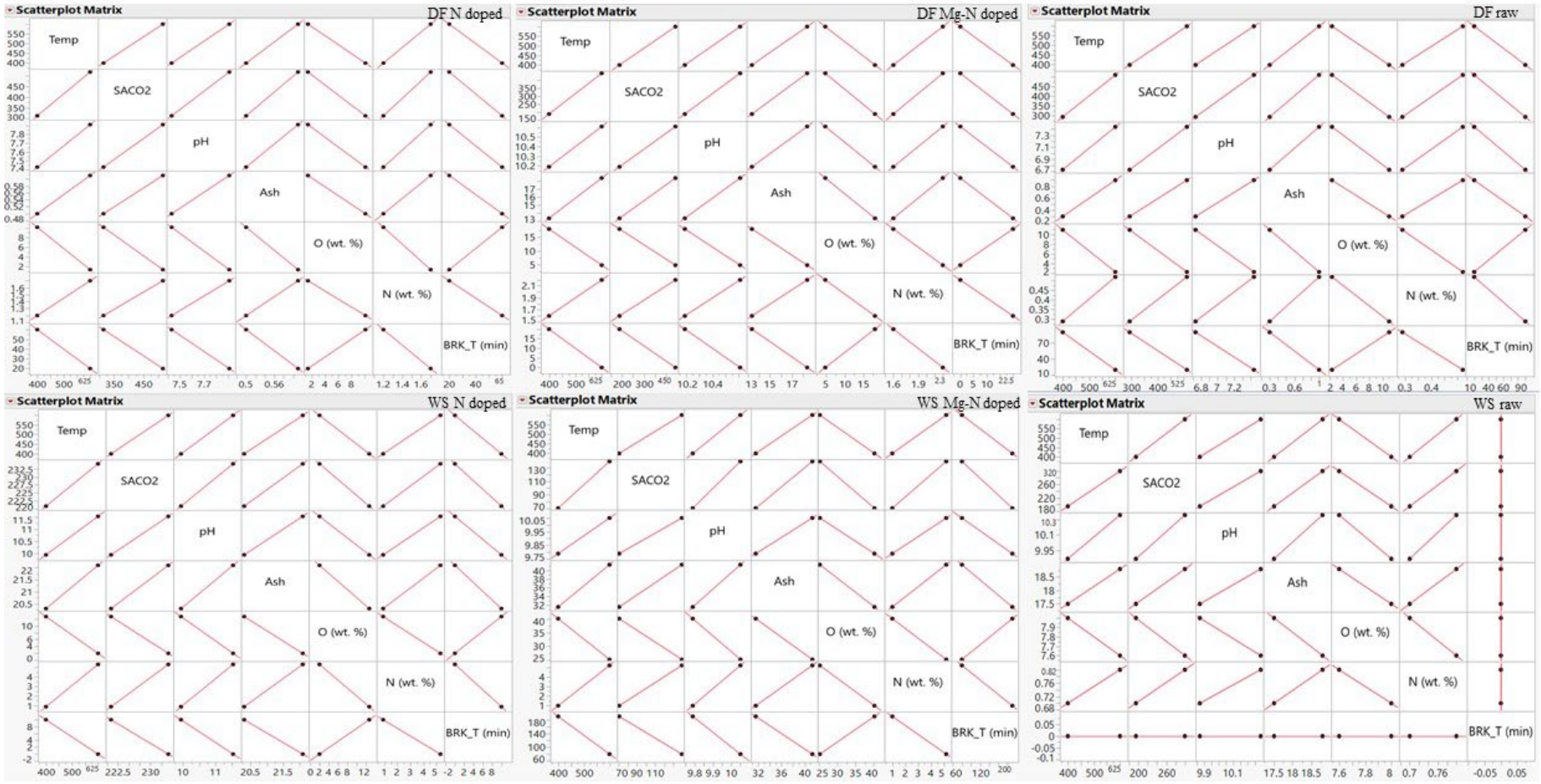

Figure A2: Scatter Plot for the correlation analysis for the NH_3 adsorption experiments.

Table A13: Correlation analysis for the DF raw biochar for the CO_2 adsorption test.

Row	Temp	SACO2	pH	Ash	N (wt. %)	BRK_T (min)
Temp	1	1	1	1	1	1
SACO2	1	1	1	1	1	1
pH	1	1	1	1	1	1
Ash	1	1	1	1	1	1
N (wt. %)	1	1	1	1	1	1
BRK_T (min)	1	1	1	1	1	1

Table A14: Correlation analysis for the DF N doped biochar for the CO_2 adsorption test.

Row	Temp	SACO2	pH	Ash	N (wt. %)	BRK_T (min)
Temp	1	1	1	1	1	-1
SACO2	1	1	1	1	1	-1
pH	1	1	1	1	1	-1
Ash	1	1	1	1	1	-1
N (wt. %)	1	1	1	1	1	-1
BRK_T (min)	-1	-1	-1	-1	-1	1

Table A15: Correlation analysis for the WS raw biochar for the CO_2 adsorption test.

Row	Temp	SACO2	pH	Ash	N (wt. %)	BRK_T (min)
Temp	1	1	1	1	1	-1
SACO2	1	1	1	1	1	-1
pH	1	1	1	1	1	-1
Ash	1	1	1	1	1	-1
N (wt. %)	1	1	1	1	1	-1
BRK_T (min)	-1	-1	-1	-1	-1	1

Table A16: Correlation analysis for the WS N doped biochar for the CO_2 adsorption test.

Row	Temp	SACO2	pH	Ash	N (wt. %)	BRK_T (min)
Temp	1	1	1	1	1	1
SACO2	1	1	1	1	1	1
pH	1	1	1	1	1	1
Ash	1	1	1	1	1	1
N (wt. %)	1	1	1	1	1	1
BRK_T (min)	1	1	1	1	1	1

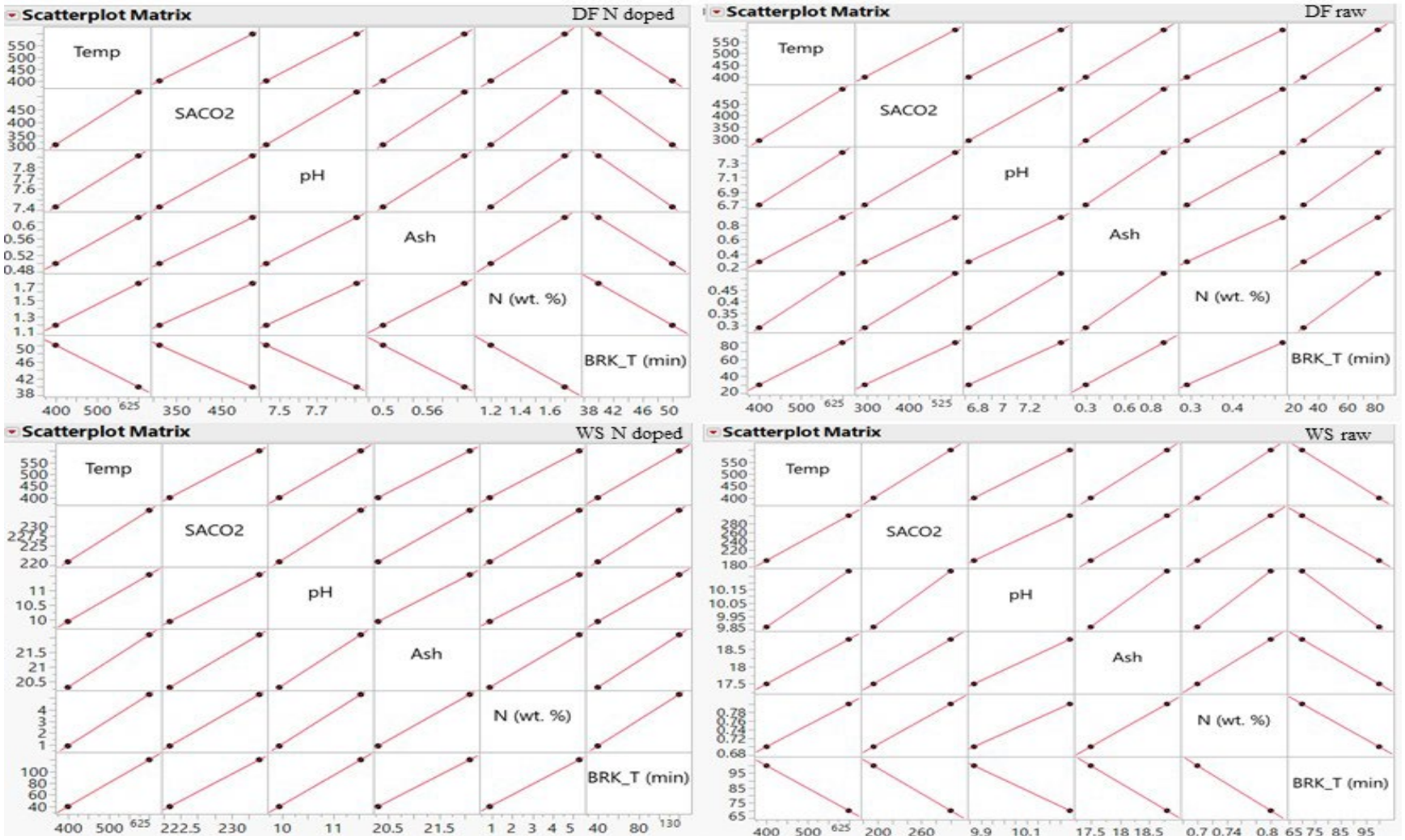

Figure A3: Scatter Plot for the correlation analysis for the CO_2 adsorption experiment.